How vortices mix

Patrice Meunier, Emmanuel Villermaux

How vortices mix

By P. Meunier and E. Villermaux

IRPHE, Université de Provence, Aix–Marseille 1
Technopôle de Château-Gombert
49, rue Frédéric Joliot-Curie 13384 Marseille Cedex 13, France

(Received 29 October 2002)

The advection of a passive scalar blob in the deformation field of an axisymmetric vortex is a simple mixing protocol for which the advection-diffusion problem is amenable to a near-exact description. The blob rolls-up in a spiral which ultimately fades away in the diluting medium. The complete transient concentration field in the spiral is accessible from the Fourier equations in a properly chosen frame. The concentration histogram of the scalar wrapped in the spiral presents unexpected singular transient features and its long time properties are discussed in connection with mixtures from the real world.

1. Introduction

A central question in scalar mixing consists in offering a satisfactory description of the histogram, or Probability Density Function (PDF) $P(c)$ of the concentration levels c of the substance being mixed. The question is particularly interesting, and relevant to many applications when the substrate is stirred since in that case molecular diffusion is altered, and in most cases enhanced, by the underlying substrate motions.

The interplay between molecular diffusion and simple deformation fields is a classical problem. It is solved in a closed form in a variety of situations such as the saddle point flow, the simple shear in two dimensions (Ranz(1979), Moffatt(1983)), in three dimensions (Villermaux & Rehab(2000)), and in the axisymmetric point vortex (Rhines & Young(1983), Flohr & Vassilicos(1997)) or spreading vortex flow (Marble(1988), Bajer et al. (2001)).

Most of the attention has focussed on the kinetics of the diffusion process in the presence of stirring motion, particularly its dependence on the substrate rate of deformation γ, and diffusion properties of the scalar (diffusivity D). Regarding the characteristic time t_s after which fluctuations start to decay from an initial scalar spatial distribution, of crucial importance is the rate at which material lines grow in time due to the substrate motions (Villermaux(2002)). If material lines grow like γt, as it is the case in a point vortex flow, the mixing time of, say, a scalar blob of initial size s_0 is $t_s \sim \gamma^{-1} Pe^{1/3}$; if material surfaces in three dimensions grow like $(\gamma t)^2$, then $t_s \sim \gamma^{-1} Pe^{1/5}$ and if material lines are exponentially stretched like $e^{\gamma t}$, then $t_s \sim (2\gamma)^{-1} \log Pe$ where $Pe = \gamma s_0^2/D$ is a Péclet number.

The times t_s given above are the relevant mixing times as soon as the inverse of the elongation rate γ^{-1} is smaller than the diffusive time of the blob constructed on its initial size s_0^2/D, that is for $Pe > 1$. In the limit $Pe \gg 1$, t_s is essentially given by the time needed to deform the blob γ^{-1} and molecular diffusion, although a crucial step in the ultimate uniformization, plays only a weak correction role in the kinetics of the process.

Experiments or numerical simulations addressing this problem quantitatively are scarce,

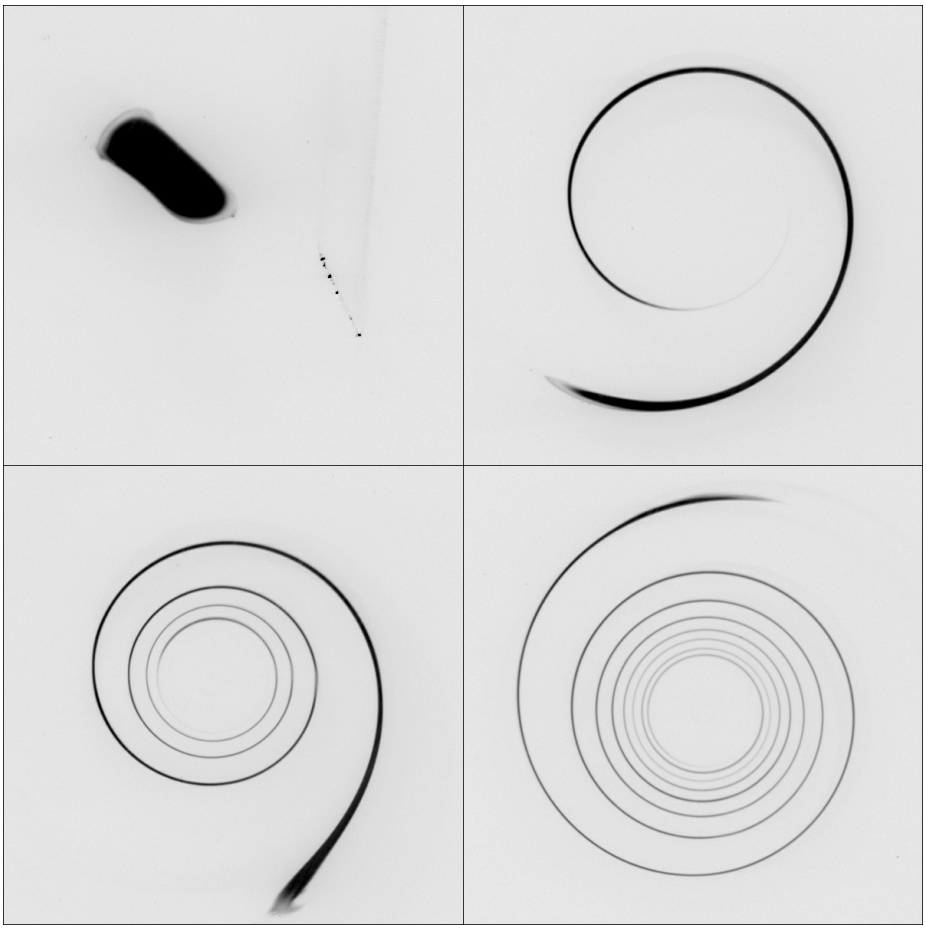

Figure 1. Roll-up of a blob of fluorescent dye in a point vortex at $t = 0$ (upper left), $t = 2$ sec (upper right), $t = 5$ sec (lower left) and $t = 10$ sec (lower right). Each picture covers a field 4.8×4.8 cm^2 wide and the circulation of the vortex is 14.2 cm^2/s. The data come from experiments described in section 2.

and are mostly limited to short times (i.e. $t \lesssim t_s$), therefore reflecting more the kinematics of the flow than its mixing properties (see, however Cetegen & Mohamad(1993) and Verzicco & Orlandi(1995)).

Based on a spatially and temporally resolved experiment, we study the mixing chronology of a blob of dye embedded in the displacement field of a diffusing, Lamb–Oseen type vortex. The process is described, from the initial segregation of the blob to a state where it is almost completely diluted in the surrounding medium, through the evolution of the spatial scalar field, and associated transient evolution of the overall concentration distribution $P(c)$.

2. A diffusive spiral

2.1. *Chronology*

The phenomenon we analyze is illustrated on Figure 1. A uniform blob of dye (the dark patch shown on Fig. 1(a))is deposed in a still transparent medium. Then a vortex is formed by the roll-up of a vortex sheet in the vicinity of the blob, which wraps around

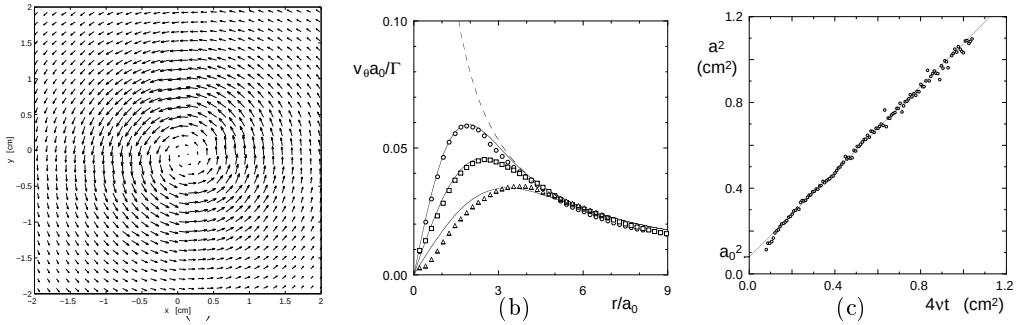

FIGURE 2. (a) Velocity field in the plane of the vortex at $t = 10$ sec. (b) Radial profiles of the azimuthal velocity measured at $t = 5$ sec ($\circ$), $t = 10$ sec ($\square$) and $t = 20$ sec ($\triangle$). Solid lines correspond to the profiles expected from a Lamb-Oseen vortex defined by (2.1) with $\Gamma = 14.2$ cm^2/s and $a_0 = 0.3$ cm. The dashed line corresponds to a point vortex defined by (3.1). (c) Core size of the Lamb-Oseen vortex measured by a least-square fit of the two-dimensional measured velocity field and compared to Eq. (2.2) (solid line).

the vortex as seen on Figure 1(b). Although it has been brought to a thin transverse size, most of the fluid particles constitutive of the blob still bear the initial concentration. The blob deforms in a spiral shape and after four turns (Fig. 1(c)), the dye concentration is no more uniform along the spiral: it is weaker near the center of the vortex where the spiral is very thin, and still close to the injection concentration in the outer region of the spiral which is thicker there. On Fig. 1(d), the spiral has made more than seven turns and is about to vanish in the diluting medium. The thickness of the spiral is fairly constant.

Molecular diffusion has clearly been enhanced by the vortex motion. The time lapse between figures 1(a) and 1(d) is 10 seconds, when the timescale of pure diffusion based on the initial size s_0 of the blob s_0^2/D is about 10^3 seconds.

2.2. *Flow field*

The vortex is formed by the impulsive flap motion of a long flat plate in a large tank of water initially at rest. The vorticity layer formed at the surface of the plate rolls-up and detaches at the plate end, producing an axisymmetric vortex which remains two-dimensional long after the dye has been mixed. A thin uniform Argon-Ion laser sheet is shed through the tank perpendicular to the plate, and the two-dimensional motion of the vortex is analyzed by Particle Image Velocimetry (PIV) using a Kodak 1008×1018 pixels digital camera aimed perpendicular to the laser sheet. Further information on the set-up and PIV techniques can be found in Meunier & Leweke(2002a) and Meunier & Leweke(2002b) respectively.

The dye is introduced, prior to the formation of the vortex, by a small tube positioned below the laser sheet, and forming a slowly ascending column of dye, aligned with the vortex axis. The dye concentration field (disodium Fluoresceine with initial concentration $c_0 \approx 10^{-3}$ mol/l) is recorded with the same camera and stored on a disk. The overall framing rate allows a complete roll-up sequence to be temporally resolved. The images are digitized on 8 bits and the resulting background subtracted grey levels are proportional to the dye concentration.

Figure 2(a) shows an example of the axisymmetric velocity field obtained by PIV after the vortex creation. The radial profiles of azimuthal velocity v_θ shown on Fig. 2(b) agree well with that of a Lamb-Oseen vortex, defined in the cylindrical coordinates $(r\,,\theta\,,z)$ by

$$v_\theta = \frac{\Gamma}{2\pi r}\left(1 - \mathrm{e}^{-r^2/a^2}\right) \tag{2.1}$$

Here, $\Gamma = 14.2\,\mathrm{cm}^2/\mathrm{s}$ is the circulation of the vortex, and a its core size. This vortex is an exact solution of the Navier-Stokes equations provided that

$$a^2 = a_0^2 + 4\nu t \tag{2.2}$$

where ν is the kinematic viscosity of the fluid, a law in close agreement with the observed growth (Fig. 2(c)), a_0 being the initial vortex radius equal to 0.3 cm.

The dashed line in Fig. 2(b) is the velocity profile of a point vortex with the same circulation, defined by (3.1). It is tangent to the measured velocity profiles for large radii ($r/a_0 > 3$).

Willing to decouple the problem of mixing from the (trivial) problem of the temporal evolution of the velocity field itself, we have systematically deposed the blob of dye far enough from the vortex core so that the velocity field remains that of a steady, point vortex, throughout the whole mixing process.

3. Concentration field along the spiral

We consider the evolution of a blob of dye of initial size s_0, in the two-dimensional, incompressible flow of a point vortex of circulation Γ (see Fig. 3a), whose azimuthal velocity is

$$v_\theta = \frac{\Gamma}{2\pi r} \tag{3.1}$$

We first describe the kinematics of the blob deformation. A fluid particle of the blob located at a distance r from the center of the vortex turns during time t by an angle θ

$$\theta(r,t) = \int_0^t \frac{v_\theta}{r}\,\mathrm{dt} = \frac{\Gamma t}{2\pi r^2} \tag{3.2}$$

A scalar strip of initial length dr, located at a distance r from the vortex center (Fig. 3(a)) is stretched so that its length equals at time t

$$\mathrm{dX} = \sqrt{\mathrm{d}r^2 + (r\mathrm{d}\theta)^2} = \mathrm{d}r\sqrt{1 + r^2\left(\frac{\mathrm{d}\theta}{\mathrm{d}r}\right)^2} = \mathrm{d}r\sqrt{1 + \frac{\Gamma^2 t^2}{\pi^2 r^4}} \tag{3.3}$$

Meanwhile, the transverse, or striation thickness $s(t)$ of the strip, in the absence of diffusion, decreases so that the surface $s(t)\mathrm{dX}$ remains constant in this two dimensional flow

$$s(t) = \frac{s_0\,\mathrm{dr}}{\mathrm{dX}} = \frac{s_0}{\sqrt{1 + \frac{\Gamma^2 t^2}{\pi^2 r^4}}} \tag{3.4}$$

We now describe the scalar dissipation of the blob. The displacement field results locally in a compression perpendicular to the strip, and in an extension along the strip. It is convenient to introduce a frame of reference (O, X, Y) whose X-axis is locally aligned

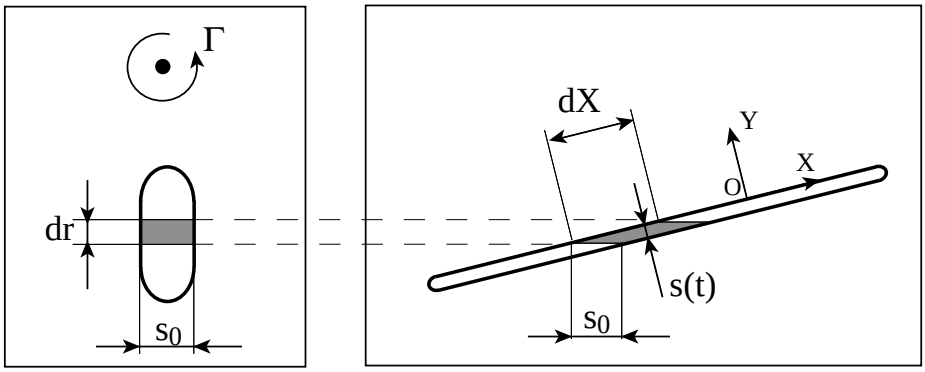

FIGURE 3. Schematic of the scalar blob elongation. (a) initial state and (b) at time t

with the spiral as shown on Fig. 3(b). In that frame, the velocity field is prescribed by the temporal evolution of the striation thickness $s(t)$ as

$$U = -\frac{X}{s}\frac{\mathrm{d}s}{\mathrm{d}t} \qquad \text{and} \qquad V = \frac{Y}{s}\frac{\mathrm{d}s}{\mathrm{d}t} \tag{3.5}$$

The evolution equation for the dye concentration c is the convection–diffusion equation in the (X, Y) coordinates

$$\frac{\partial c}{\partial t} + U\frac{\partial c}{\partial X} + V\frac{\partial c}{\partial Y} = D\left(\frac{\partial^2 c}{\partial X^2} + \frac{\partial^2 c}{\partial Y^2}\right) \tag{3.6}$$

The ratio of the two convective terms $V\partial c/\partial Y$ and $U\partial c/\partial X$ is in magnitude proportional to the strip aspect ratio $1 + (\Gamma^2 t^2)/(\pi^2 r^4)$: the concentration varies more slowly along the spiral than in its transverse direction for $\Gamma t/r^2 > 1$ so that Eq. (3.6) becomes

$$\frac{\partial c}{\partial t} + \frac{Y}{s}\frac{\mathrm{d}s}{\mathrm{d}t}\frac{\partial c}{\partial Y} = D\,\frac{\partial^2 c}{\partial Y^2} \tag{3.7}$$

A change of variables (see e.g. Ranz(1979), Marble(1988), Villermaux & Rehab(2000)) consisting in counting transverse distances in units of the striation thickness $s(t)$ and time in units of the current diffusion time $s(t)^2/D$ transforms Eq. (3.7) into a simple diffusion equation

$$\text{with} \quad \xi = \frac{Y}{s(t)} \quad \text{and} \quad \tau(r) = \int_0^t \frac{D\mathrm{d}t'}{s(t')^2} = \frac{Dt}{s_0^2} + \frac{D\Gamma^2 t^3}{3\pi^2 r^4 s_0^2} \quad \text{giving} \quad \frac{\partial c}{\partial \tau} = \frac{\partial^2 c}{\partial \xi^2} \tag{3.8}$$

If c_0 is the initial concentration of the dye, the initial conditions at $\tau = 0$ are

$$\begin{cases} c = c_0 & \text{for} \quad |\xi| < 1/2 \\ c = 0 & \text{for} \quad |\xi| > 1/2 \end{cases} \tag{3.9}$$

The concentration profile at any time and radial position along the spiral is

$$c(\xi, \tau) = \frac{c_0}{2}\left[\mathrm{erf}\left(\frac{\xi + 1/2}{2\sqrt{\tau}}\right) - \mathrm{erf}\left(\frac{\xi - 1/2}{2\sqrt{\tau}}\right)\right] \tag{3.10}$$

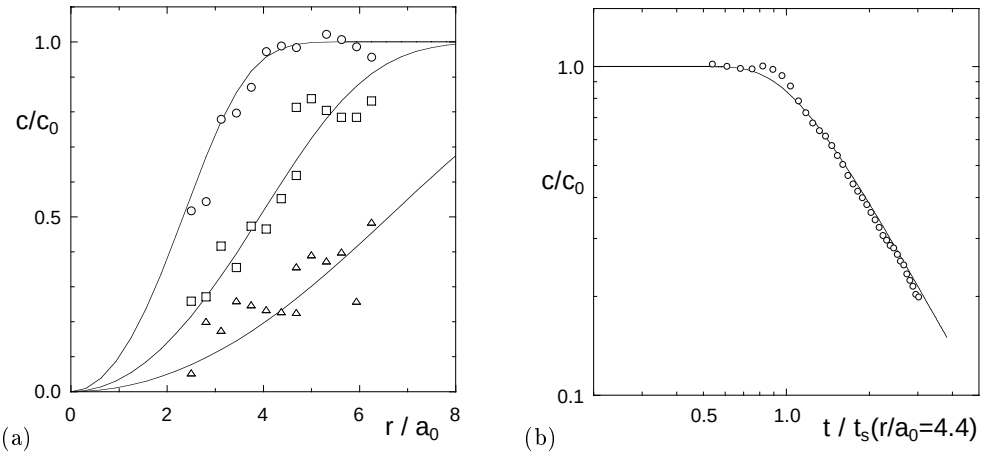

FIGURE 4. Comparison of the maximal dye concentrations obtained experimentally (symbols) and theoretically (solid lines) by Eq.(3.11). (a) Radial dependence at $t = 5\,\mathrm{sec}$ ($\circ$), $t = 10\,\mathrm{sec}$ ($\Box$) and $t = 20\,\mathrm{sec}$ ($\triangle$). (b) Temporal dependence for $r/a_0 = 4.4$

The maximal concentration is obtained at the profile center $\xi = 0$

$$c_M(r,t) = c_0\,\mathrm{erf}\left(\frac{1}{4\sqrt{\tau}}\right) = c_0\,\mathrm{erf}\left(\frac{1}{4\sqrt{\frac{Dt}{s_0^2} + \frac{D\Gamma^2 t^3}{3\pi^2 r^4 s_0^2}}}\right) \tag{3.11}$$

This relation can be examined from the experiment ($\Gamma = 14.2\ \mathrm{cm}^2/\mathrm{s}$, $D = 5 \times 10^{-6}$ cm^2/s and $s_0 \approx 0.22$ cm). Figure 4(a) shows the maximal dye concentrations as a function of the radius r at a fixed time, for three different times. The concentration falls to zero more rapidly closer to the spiral center since the rate of elongation is higher there (see Eq. (3.3)).

Conversely, the temporal evolution of the concentration at a fixed $r-$location is constant (Fig. 4(b)) up to the mixing time $t_s(r)$. This time makes the argument of the error function in Eq. (3.11) of order unity i.e. $\tau = O(1)$

$$t_s(r) = \frac{r^2}{\Gamma}\left(\frac{3\pi^2}{16}\right)^{1/3}\left(\frac{s_0}{r}\right)^{2/3}\left(\frac{\Gamma}{D}\right)^{1/3} \tag{3.12}$$

and displays the expected Péclet number dependence $Pe^{1/3}$, with $Pe = \Gamma/D$ characteristic of flows where material lines grow asymptotically linearly in time (see Eq. (3.3)). After the mixing time, the maximal concentration c_M decreases like $t^{-3/2}$, in close agreement with the trend shown on Fig. 4(b).

4. Probability Density Function

If A is the total surface area of the spiral bearing a non-zero concentration level, the Probability Density Function (PDF) of the scalar $P(c)$ is the fraction of the total area whose concentration lies in the interval $[c,\ c+\mathrm{d}c]$. It is convenient to compute $P(c)$ in the (r,ξ) coordinates where ξ is defined in (3.8) so that with $\mathrm{d}X = \sqrt{1 + (\Gamma^2 t^2)/(\pi^2 r^4)}\ \mathrm{d}r$ and $\mathrm{d}Y = s\,\mathrm{d}\xi = s_0\,\mathrm{d}\xi/\sqrt{1 + (\Gamma^2 t^2)/(\pi^2 r^4)}$, one has

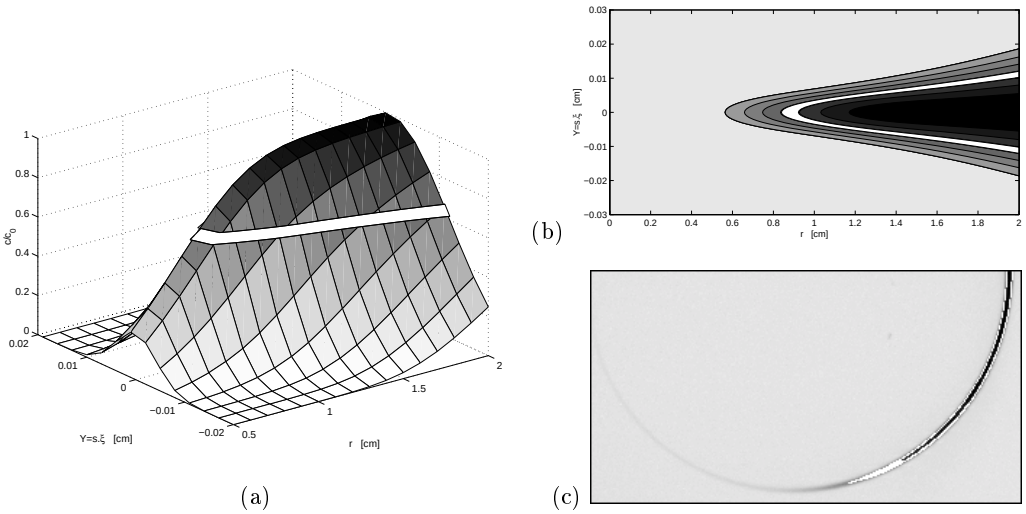

(a) (b) (c)

FIGURE 5. (a) Perspective view and (b) contour plot of the concentration profile given in Eq. (4.2). The white band corresponds to an iso-concentration $c/c_0 = 0.6$. (c) Zoom of the end of the spiral on Fig. 1 and same construction.

$$P(c)\mathrm{dc} = \iint_{c(X,Y)\in[c,\ c+\mathrm{dc}]} \frac{\mathrm{dX\ dY}}{A} = \iint_{c(r,\xi)\in[c,\ c+\mathrm{dc}]} \frac{s_0\ \mathrm{dr\ d}\xi}{A} \tag{4.1}$$

The scalar spatial distribution is given in Eq. (3.10) as the difference of two error functions. However, after the mixing time, that is when the spiral thickness is very thin, this difference approximates the derivative of the error function, providing a Gaussian concentration profile

$$c(\xi, r) = c_0\ \mathrm{erf}\left(\frac{1}{4\sqrt{\tau(r)}}\right) \mathrm{e}^{-\xi^2/2\sigma_\xi^2} \tag{4.2}$$

where $\tau(r)$ is given by Eq. (3.8) and $\sigma_\xi(r)$ is the standard deviation of the original profile $c(Y)$ given in Eq. (3.10)

$$\sigma^2 = \frac{\int Y^2 c(Y)\ \mathrm{dY}}{\int c(Y)\ \mathrm{dY}} = s^2(t)\frac{\int \xi^2 c(\xi)\ \mathrm{d}\xi}{\int c(\xi)\ \mathrm{d}\xi} = s^2(t)\frac{1+24\tau(r)}{12}, \quad \text{or} \quad \sigma_\xi^2 = \frac{1+24\tau(r)}{12} \tag{4.3}$$

Note that the 'spiral thickness' σ first decreases as t^{-1}, reaches a minimum at $t = t_s$ and re-increases as $t^{1/2}$ after the mixing time, when the spiral is locally nearly parallel to the vortex streamlines.

The shape of the iso-concentration lines $c(r\,, \xi) = c$ in the (r, ξ) plane is shown in Fig. 5

$$\xi(r, c) = \pm\sigma_\xi(r)\sqrt{2\log\left[\mathrm{erf}\left(1/4\sqrt{\tau(r)}\right)\right] - 2\log(c/c_0)} \tag{4.4}$$

This curve is defined for $r > r_1^*(c)$ only, that is above the smallest radius bearing the concentration c at time t

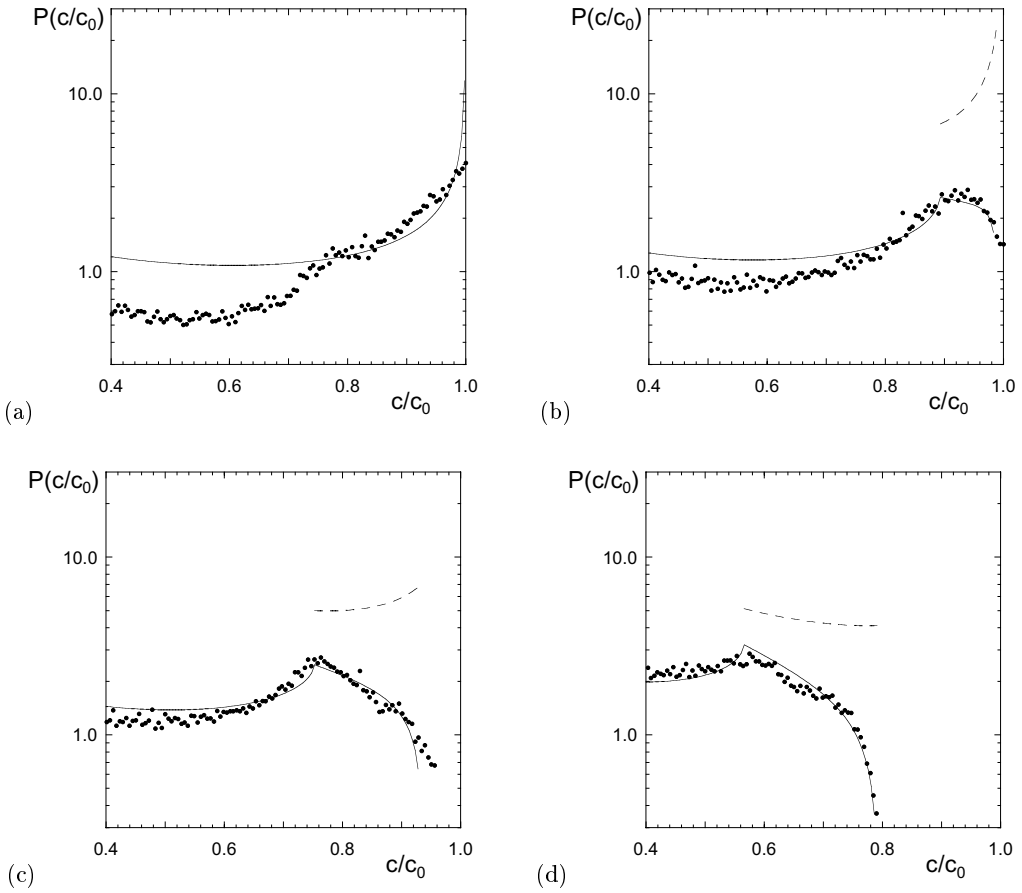

FIGURE 6. Probability Density Functions at (a) $t = 5\,\mathrm{sec}$, (b) $t = 8\,\mathrm{sec}$, (c) $t = 10\,\mathrm{sec}$ and (d) $t = 13\,\mathrm{sec}$. Solid lines correspond to the theoretical prediction given by Eq. (4.6) and dashed lines correspond to the PDF of the spatial maxima of concentration, defined by Eq. (4.7).

$$r_1^*(c) = \left[\frac{16}{3\pi^2}\,\frac{D\Gamma^2 t^3}{s_0^2\left[\mathrm{erf}^{-1}(c/c_0)\right]^{-2} - 16Dt}\right]^{1/4} \tag{4.5}$$

If the scalar blob was initially delimited between the radii r_1 and r_2, the concentration PDF is

$$P(c) = \frac{2s_0}{A}\int_{\max[r_1, r_1^*(c)]}^{r_2} \left|\frac{\partial c}{\partial \xi}\right|^{-1} \mathrm{dr} \tag{4.6}$$

The concentration profile across the spiral, and the evolution of the maximal concentration along the spiral set the global PDF.

The above relation is compared on Fig. 6 with the experimental histograms recorded with a blob initially located between $r_1 = 1.65\,\mathrm{cm}$ and $r_2 = 2.1\,\mathrm{cm}$. At early stages, (Fig. 6a), as long as most of the fluid particles constitutive of the spiral have not reached the mixing time yet, the PDF is that of a Gaussian spatial profile $1/c\sqrt{\log(c/c_M)}$ with $c_M = c_0$ displaying a characteristic $\cup$ shape.

As soon as diffusion becomes effective, the PDF nucleates a cusp located at the maximal concentration $c_M(r_1)$ obtained at the inner end of the spiral. The shape of the PDF for $c_M(r_1) < c < c_M(r_2)$ results from the superposition of the right branches of the $\cup$ shaped distributions parameterized by $c_M(r)$ with $r_1 < r < r_2$ (Fig. 6b,c,d) and weighted by the probability of finding the maximal concentration c_M, namely $Q(c_M)$. This distribution is the fraction of the spiral length dX whose concentration is in the interval $[c_M,\ c_M + \mathrm{dc_M}]$

$$Q(c_M) = \frac{1}{L}\left|\frac{\mathrm{dc_M}}{\mathrm{dX}}\right|^{-1} \tag{4.7}$$

where L is the spiral length $L = \int_{r_1}^{r_2} \mathrm{dX}$. It is defined in the range $[c_M(r_1),\ c_M(r_2)]$ and shown as the dotted line on Fig. 6. At short times, $P(c)$ and $Q(c_M)$ are very different because the low concentration levels at a small radii r and $\xi = 0$ are as numerous as the same levels at the edges of the Gaussian transverse profile ($\xi \neq 0$) at a higher r. The spatial distribution $c(\xi)$ contaminates the whole distribution $P(c)$, inducing the characteristic $\cup$ shape. At later stages (Fig. 6d), the low levels of concentration from the edges of the Gaussian profile at large radii are rare in comparison to those at the center of the spiral and $\xi = 0$. Therefore, $Q(c_M)$ becomes a decreasing function of c and gets closer to $P(c)$. In the final stages, when $\Gamma t/r^2 \gg 1$ and for $t_s(r) > 1$ for all r, these two distributions are both given by

$$P(c) \approx Q(c_M = c) \sim \left(\frac{\tilde{r}^4 s_0^2}{D\Gamma^2 t^3}\right)^{1/4} \frac{1}{c^{3/2}} \tag{4.8}$$

where $\tilde{r}$ stands for $(1/r_1 + 1/r_2)^{-1}$.

5. Conclusions and implications

In the simple displacement field of a two-dimensional vortex, a direct connection exists between the microscopic equations of diffusion, and the resulting global statistics of the mixture through the scalar concentration PDF $P(c)$ which, therefore, appears as a reformulation of the microscopic convection–diffusion problem.

This one-to-one connection is possible because the flow solely results in a spatial mapping of the fluid particles with no interaction between the particles themselves. The concentration of a given fluid element evolves due to molecular diffusion and not because it interacts with a nearby element; indeed, the arms of the spiral never reconnect. This situation would lead to a completely different route for the evolution of $P(c)$. It is, to this respect, useful to learn that the distribution $Q(c_M)$ tends asymptotically towards $P(c)$, a hidden assumption made when considering mixtures evolution by particle interaction (Curl(1963), Pope(1985), Pumir et al. (1991), Villermaux(2002)).

The simple stirring protocol considered here also provides an exact estimation of the scalar dissipation rate $\chi = -\frac{\mathrm{d}}{\mathrm{dt}}\langle c^2\rangle = 2D\langle(\nabla c)^2\rangle$, a quantity sometimes modeled in an ad-hoc way. Here $\langle\cdot\rangle$ denotes a spatial integration, therefore

$$\chi = 2D\int_{r_1}^{r_2} \frac{\mathrm{dX}}{s(t)} \int_{-\infty}^{+\infty} \left(\frac{\partial c}{\partial \xi}\right)^2 \mathrm{d}\xi \tag{5.1}$$

With $c(\xi)$ given in Eq. (3.10) and $\int_{-\infty}^{+\infty}\left(\frac{\partial c}{\partial \xi}\right)^2 \mathrm{d}\xi \sim \frac{1-e^{-1/8\tau(r)}}{\sqrt{\tau(r)}}$, one sees that as soon as $\Gamma t/r^2 > 1$

$$\begin{cases} \chi \sim \frac{\Gamma}{s_0}\sqrt{Dt} & \text{when} \quad t < t_s(r) \quad \text{for all } r \\ \chi \sim \frac{s_0}{\sqrt{D\Gamma}} t^{-5/2} & \text{when} \quad t > t_s(r) \quad \text{for all } r \end{cases} \tag{5.2}$$

As long as most of the fluid particles constitutive of the spiral have not reached the mixing time (i.e. while $t < t_s(r)$ and $\tau(r) \ll 1$), χ reflects both the diffusive smoothing ($\sim 1/\sqrt{Dt}$) at the edges of the concentration profile $c(\xi)$, and the increase of the concentration support length ($\sim \Gamma t$). When the mixing time has been reached all along the spiral (i.e. when $t > t_s(r)$ and $\tau(r) > 1$), the maximal concentration c_M decays as $t^{-3/2}$, the profile thickness σ re-increases by pure diffusion like $t^{1/2}$ and the spiral length still increases like Γt, thus, since $\chi \sim (c_M/\sigma)^2 \sigma \Gamma t$, providing the $t^{-5/2}$ time dependence in Eq. (5.2).

Acknowledgments: We thank Dr. Thomas Leweke for encouragements, and useful discussions.

REFERENCES

BAJER, K., BASSOM, A. P. & GILBERT, A. D. 2001 Accelerated diffusion in the centre of a vortex. *J. Fluid Mech.* **437**, 395–411.

CETEGEN, B. M. & MOHAMAD, N. 1993 Experiments on liquid mixing and reaction in a vortex. *J. Fluid Mech.* **249**, 391–414.

CURL, R. L. 1963 Dispersed phase mixing: I. theory and effect in simple reactors. *AIChE J.* **9**, 175–181.

FLOHR, P. & VASSILICOS, J. C. 1997 Accelerated scalar dissipation in a vortex. *J. Fluid Mech.* **348**, 295–317.

MARBLE, F. E. 1988 Mixing, diffusion and chemical reaction of liquids in a vortex field. In *Chemical Reactivity in Liquids: Fundamental Aspects* (ed. M. Moreau & P. Turq), pp. 581–596. Plenum.

MEUNIER, P. & LEWEKE, T. 2002a Elliptic instability of a co-rotating vortex pair. Submitted to *J. Fluid Mech.*

MEUNIER, P. & LEWEKE, T. 2002b Analysis and optimization of the error caused by high velocity gradients in PIV. Submitted to *Exp. Fluids.*

MOFFATT, H. K. 1983 Transport effects associated with turbulence with particular attention to the influence of helicity. *Rep. Prog. Phys.* **46**, 621–664.

POPE, S. B. 1985 Pdf methods for turbulent reacting flows. *Prog. Energy Combust. Sci.* **11**, 119–192.

PUMIR, A., SHRAIMAN, B. I. & SIGGIA, E. D. 1991 Exponential tails and random advection. *Phys. Rev. Letters* **66**, 2984–2987.

RANZ, W. E. 1979 Application of a stretch model to mixing, diffusion and reaction in laminar and turbulent flows. *AIChE J.* **25**, 41–47.

RHINES, P. B. & YOUNG, W. R. 1983 How rapidly is a passive scalar mixed within closed streamlines. *J. Fluid Mech.* **133**, 133–145.

VERZICCO, R. & ORLANDI, P. 1995 Mixedness in the formation of a vortex ring. *Phys. Fluids* **7** (6), 1513–1515.

VILLERMAUX, E. 2002 Mixing as an aggregation process. In *Turbulent Mixing and Combustion* (ed. A. Pollard & S. Candel), pp. 1–21. Kluwer Academic Publishers.

VILLERMAUX, E. & REHAB, H. 2000 Mixing in coaxial jets. *J. Fluid Mech.* **425**, 161–185.